Modeling of Short-Term Tidal Power Fluctuations

Guðrún Margrét Jónsdóttir *IEEE, Student Member* and Federico Milano, *Fellow, IEEE*

***Abstract*— This paper proposes the utilization of stochastic differential equations to model short-term fluctuations of tidal currents. Two relevant environmental scenarios are considered, namely, with and without waves. As opposed to the models currently available in the literature, the proposed models are based on measurement data and are shown to capture the statistical properties, i.e. the autocorrelation and the probability distribution, of such data for both scenarios. The proposed models can be readily incorporated in tidal turbine models for short-term stability analysis of power systems.**

***Index Terms*— Tidal generation, tidal current, turbulence, waves, stochastic differential equations.**

I. Introduction

A. Motivation

The potential of marine and tidal currents for electric power generation is widely recognized [1], [2] although multiple techno-economic issues have still to be solved. Historical projects in this area include, for example, the SeaGen project in Strangford Lough, Northern Ireland, the Deepgen project by Tidal Generation Ltd. and a project by ANDRITZ HYDRO Hammerfest deployed at the European Marine Energy Centre (EMEC) tidal test site. Notable recent activities are ongoing within the MeyGen project (Pentland Firth, Scotland) [3] and the Nova Innovation tidal array (Shetland, Scotland), along with operations led by Orbital (Orkney, Scotland) and Sabella (Fromveur Passage, France). These projects demonstrate that tidal stream generation is a viable source of renewable energy.

Tidal currents have a high long-term predictability compared to other prominent renewable energy sources, e.g. wind and solar. However, short-term fluctuations (seconds to minutes) in the current are less predictable. These short-term fluctuations are caused by turbulence and waves and they can negatively impact the power quality and the stability of power systems including tidal generation. In [4], the fluctuations in the power output of the SeaGen tidal generators are studied. There it is shown that the power output of a 600 kW turbine can ramp up/down by 10 kW in a matter of seconds. Experience from the ReDAPT tidal project (ETI, UK) shows levels of power fluctuations far greater, with routine fluctuations, particularly during winter months, of $20 - 30$ % of rated power per wave-cycle. Thus, understanding and characterizing these fluctuations is essential for the development, design and operation of tidal power plants. The modeling of these fluctuations based on measured data is the subject of this paper.

G. .M. Jónsdóttir and F. Milano are with the School of Electrical & Electronic Engineering, University College Dublin, Ireland. E-mails: gudrun.jonsdottir@ucdconnect.ie, federico.milano@ucd.ie

This work is supported by the Science Foundation Ireland, by funding G. .M. Jónsdóttir and F. Milano under project AMPSAS, Investigator Programme, Grant No. SFI/15/IA/3074.

B. Literature Review

Several studies have aimed to characterize the current fluctuations due to turbulance [5]–[9]. In [5] the turbulence intensity within the bottom boundary layer at a height of 5 m is studied and is measured to be $12 - 13$ % in the tidal channel of the Sound of Islay, Scotland. A study conducted within the Puget Sound, Washington state, USA reports the turbulence intensity at approximately the same height as 10 % [6]. In [9] the turbulence intensity was shown to exhibit strong dependence on tide direction (between flood and ebb tides) and water depth. In [7] the current fluctuations with and without waves present are studied based on measurements from the English Channel, France. These studies provide valuable understanding of the statistical properties of these current fluctuations.

In tidal system studies for their integration into power systems, the fluctuations have typically been modeled as purely turbulent [10] or as dominated by waves, in particular swell waves [11]–[14]. Swell waves have been characterized as the biggest cause of fluctuations and multiple publications have addressed the damping of said fluctuations using storage or other additional control [11]–[14]. These publications model the swells using the first-order Stokes model coupled with the JONSWAP spectrum [15], [16]. This model is widely used in ocean engineering for modeling wind and swell waves. However, the model is not specifically built to model waves in sites with strong tidal flows, that is where tidal turbines are likely to be installed. Additionally, such models do not consider the coupling of the turbulence and waves. Therefore, these studies might over- or under-estimate the effect of waves on the tidal current and thereby the control/storage needed alongside the tidal turbine.

C. Contributions

This paper aims to identify how tidal current fluctuations differ for scenarios with and without waves. The models are defined are based on actual measurement data and are thus able to capture the statistical properties of the current speed fluctuations for both scenarios. These models are constructed using Stochastic Differential Equations (SDEs) and can be readily integrated into time-domain simulations of power systems. Finally, the proposed model is compared to the first-order Stokes model coupled with the JONSWAP spectrum through the equivalent power output of the turbine.

D. Organisation

The remainder of this paper is organized as follows. Section II outlines SDEs and Section III describes the SDE-based modeling method used to model the current fluctuations. Section IV illustrates the measurement data utilised to set up

SDE-based models. The generation of synthetic tidal current trajectories using the proposed model is discussed in Section V and the statistical properties of the modeled current compared to those of measurement data. In Section VI, the tidal turbine power output of the proposed model is compared to that of a model from the literature. Finally, Section VII draws conclusions and outlines future work.

II. Outline of Stochastic Differential Equations

Stochastic Differential Equations (SDEs) are a prominent mathematical modeling technique and have been utilized in previous power systems studies, e.g. for modeling loads [17], wind [18], [19] and solar [20], [21].

A generic one-dimensional SDE has the form:

$$dX(t) = a(t, X(t))dt + b(t, X(t))dW(t), \quad X(t_0) = X_0, \tag{1}$$

where $a(t, X(t))$ and $b(t, X(t))$ are referred to as the drift and diffusion term of the SDE, respectively and are continuous functions. $W(t)$ represents the stochastic component driving the SDE. Typically, this component is a Wiener process, $\{W(t), t > 0\}$, which is a random function characterized by the following properties:

1) $W(0) = 0$, with probability 1.
2) The function $t \mapsto W(t)$ is continuous in t.
3) If $t_1 \neq t_2$, then $W(t_1)$ and $W(t_2)$ are independent.
4) For $\forall t_i \geq 0$, all increments, $\Delta W_i = W(t_{i+1}) - W(t_i)$, are normally distributed, with mean 0 and variance $h = t_{i+1} - t_i$, i.e., $\Delta W_i \sim \mathcal{N}(0, h)$.

Wiener processes cannot be integrated in the conventional Riemann-Stieltjes sense. This is because they are not bounded and the limit $\lim_{x\to 0}(W(t+\Delta t)-W(t))/\Delta t$ does not exist. A specific stochastic integral has to be defined to solve the SDE in (1). There are several different ways to interpret stochastic integrals. The most widely used approach is the Itô integral, which is also the approach used in this paper. An in-depth discussion on SDEs is outside the scope of this paper. The interested reader is referred to [22] for details on SDE theory and numerical methods.

The Ornstein-Uhlenbeck (OU) process is one of the most widely known SDEs because of its simplicity and versatility. It has a Gaussian probability distribution and exhibits mean reversion, i.e. it drifts towards its mean value at an exponential rate. Moreover, the OU process has a bounded variance which makes it suitable to model physical processes such as tidal current fluctuations.

The following 2-dimensional OU is utilized as the building block of the proposed method to synthesize tidal current speed models:

$$\begin{bmatrix} dX(t) \\ dY(t) \end{bmatrix} = \begin{bmatrix} -\kappa & -\psi \\ \psi & -\kappa \end{bmatrix} \begin{bmatrix} X(t) \\ Y(t) \end{bmatrix} dt + \begin{bmatrix} \upsilon \\ 0 \end{bmatrix} dW(t), \tag{2}$$

where $\kappa > 0$, $\upsilon > 0$, $\psi \geq 0$ and $W(t)$ is a standard Wiener process. The correlation matrix of the SDE in (2) is:

$$\begin{aligned} \boldsymbol{R}(\tau) &= \mathbb{E}\begin{bmatrix} X(t+\tau) \\ Y(t+\tau) \end{bmatrix} \begin{bmatrix} X(t) & Y(t) \end{bmatrix} \\ &= \exp(-\kappa\tau) \begin{bmatrix} \cos(\psi\tau) & -\sin(\psi\tau) \\ \sin(\psi\tau) & \cos(\psi\tau) \end{bmatrix}. \end{aligned} \tag{3}$$

Thus, the process $X(t)$ has the autocorrelation:

$$R_X(\tau) = \exp(-\kappa\tau)\cos(\psi\tau). \tag{4}$$

In stationary conditions, $X(t)$ is Gaussian distributed with zero mean and variance $\upsilon^2/(2\kappa)$. For $\psi = 0$, $X(t)$ and $Y(t)$ are decoupled and $X(t)$ becomes a conventional 1-dimensional OU process:

$$dX(t) = -\kappa X(t)dt + \upsilon dW(t), \tag{5}$$

with an exponentially decaying autocorrelation:

$$R_X(\tau) = \exp(-\kappa\tau). \tag{6}$$

The $X(t)$ component of the process in (2) is used in the remainder of this paper for building the tidal current speed models discussed in the following section.

III. Modeling of Tidal Current Speed

Tidal generators extract energy from the ocean movement due to the tidal phenomenon. This phenomenon is due to the changing gravitational pull of the sun and moon in respect to the earth's oceans. It causes large bodies of water to move towards and away from the shore. These fluctuations are site specific and each location will experience diurnal tides (one high, one low in a tidal day), semi-diurnal tides (two high, two low in a tidal day) or a mixture of the two. Tides can be predicted far in advance and with a high degree of accuracy. The modeling and prediction of these variations in the tidal current due to the tidal phenomenon has been well defined [23]. However, the focus of this paper is the short-term behavior of tidal currents and, hence, the predicted average tidal current is represented as a constant u_0, over 10-minute intervals, throughout this paper [1].

Tidal currents are subject to short-term fluctuations within seconds to minutes. The fluctuations are due to turbulence caused by bottom and side friction as well as waves which can be local wind waves and/or remote swell waves. The modeling of these fluctuations in the current speed are of interest in this paper. The total tidal current speed is modeled as:

$$u_{\text{tidal}}(t) = u_0 + \eta(t), \tag{7}$$

where $\eta(t)$ represents the current speed fluctuations. To model these fluctuations, we adapt the SDE-based approach that was originally proposed in [19] to model wind speed fluctuations. This approach can capture an arbitrary autocorrelation and probability distribution. For simplicity but without lack of generality, we assume that the probability distribution is Gaussian. This assumption is reasonable for the short-term analysis and is also not restrictive as the memoryless transformation utilized in the procedure proposed in [19] can be readily implemented to capture any probability distribution.

The method consists in the superposition of OU processes, as defined in (2) to capture the desired autocorrelation. Thus, $\eta(t)$ is a stochastic process defined as the weighted sum of n SDE processes:

$$\eta(t) = \sum_{i=1}^{n} \sqrt{w_i}\, X_i(t), \tag{8}$$

where $X_i(t)$, $i = 1, \dots n$, are SDE processes with autocorrelations $R_{X_i}(\tau)$, $w_i > 0$ and $\sum_{i=1}^{n} w_i = 1$. If all n processes have an identical Gaussian probability distribution $\mathcal{N}(\mu_X, \sigma_X^2)$, the stochastic process $\eta(t)$ has the same Gaussian probability distribution, $\mathcal{N}(\mu_X, \sigma_X^2)$, and an autocorrelation which is a weighted sum of the autocorrelation functions of the n SDE processes, that is:

$$R_\eta(\tau) = \sum_{i=1}^{n} w_i R_{X_i}(\tau). \tag{9}$$

If the n SDE processes in (8) are $X(t)$ processes as in (2), the resulting autocorrelation of $\eta(t)$ is a weighted sum of damped sinusoidal and decaying exponential functions and (9) can be rewritten as:

$$R_\eta(\tau) = \sum_{i=1}^{n} w_i \exp(-\kappa_i \tau) \cos(\psi_i \tau). \tag{10}$$

Hence, the superposition of SDE processes allows capturing any autocorrelation that can be modeled as a weighted sum of exponential and/or sinusoidal autocorrelation. If the autocorrelation does not show a periodic behavior, then $\psi_i = 0$, $\forall i = 1, \dots, n$ (see the process defined in (5)).

IV. Data Analysis

This section presents the measured tidal current speed data used to validate the proposed model presented in Section III. The current speed data were gathered during the Reliable Data Acquisition Platform for Tidal project (ReDAPT) in the European Marine Energy Centre (EMEC) tidal test site in Orkney, UK. The data is publicly available from [24]. The measurements are collected using a single-beam acoustic Doppler profiler deployed at the nose of the test Deep-Gen IV tidal turbine. It measures the velocity directly along the stream-wise axis. The provided velocity profiles have cell sizes of 0.5 m. The measured data analyzed in this paper is the stream-wise tidal current speed measured 10 m upstream from the turbine at hub height. Further information on field measurement techniques and subsequent data processing are discussed in [9].

Two sets of data are analyzed, representing the two following scenarios:

- *Scenario 1*: The short-term fluctuations are exclusively due to turbulence. Waves are not considered.
- *Scenario 2*: The fluctuations are both due to turbulence and waves. The most significant wave height is $H_s = 1.9$ m and the peak period is $T_p = 9$ s.

Further details on each scenario are provided in Table I.

TABLE I: Details on the Scenario 1 and 2 data sets.

Scenario	Dates	Time	Sampling rate	Sea state
1	2014/08/09	14:00-18:40	2 Hz	No waves
2	2014/11/11	21:00-08:55	4 Hz	Waves
	2014/11/12			

An example of the measured time series for Scenario 1 is shown in Fig. 1.a (grey line), where a trend in the tidal current is noticeable. This trend is due to the tidal phenomenon. As the aim of this study is to model the short-term variations (in the seconds to minutes time scale) this trend is removed from the data. To identify the trend the two-sided rolling mean of the time series is used. The two-sided rolling mean of a time series y_t is defined as:

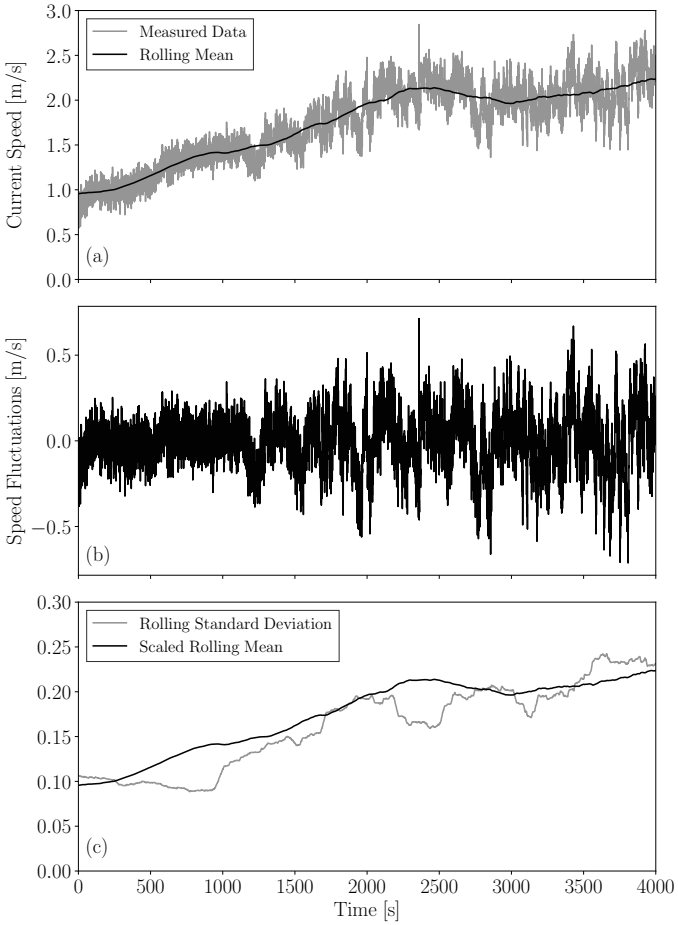

Fig. 1: (a) The measured stream wise tidal current speed (Scenario 1) and the rolling two-sided mean derived using (11). (b) The current speed fluctuations derived using (12). (c) The rolling standard deviation and the scaled rolling mean ($0.1 z_t$).

$$z_t = \frac{1}{2m+1} \sum_{j=-m}^{m} y_{t-j}, \tag{11}$$

where m is the smoothing parameter that defines the window to average over. In this case y_t is the Scenario 1 time-series. The two-sided rolling mean of the measured time-series where $m = 10$ min is shown in Fig. 1.a (black line). The measured stochastic process to be modeled in this paper is:

$$x_t = y_t - z_t, \tag{12}$$

which represents the measured tidal current speed where the trend has been removed. In this way, the short-term fluctuations of the current speed are 'isolated'. Figure 1.b shows that the standard deviation of the fluctuations is proportional to the average tidal current. This effect has also been discussed in the literature [5]–[8]. Figure 1.c shows the rolling standard deviation of the current speed fluctuations (gray line) and

the scaled down rolling mean ($0.1z_t$). This demonstrates their correlation. In the remainder of the paper, thus, we assume that the standard deviation of the fluctuations is close to $10\ \%$ of the tidal current speed.

V. Synthetic Tidal Current Trajectories

In this section, the modeling approach outlined in Section III is used to model the scenarios presented in Section IV. To define the parameters of the model for each scenario, the fitting procedure discussed in [19] is used. An overview of the fitting procedure is provided in Section V-A, whereas, in Section V-B, the model simulation procedure is outlined and the simulated time-series are compared to the measured data through their statistical properties.

A. Fitting to Data

The SDE-based modeling procedure presented in Section III consists in fitting the model to measurement data based on their statistical properties. The result of the fitting procedure is the determination of the parameters of a set of SDEs that matches the autocorrelation and the probability distribution of the original data. The probability distribution describes all the possible values and likelihoods that the process can take within a given range. The autocorrelation is a measure of how the stochastic process evolves over time. That is, the autocorrelation gives a measure of the relationship between the processes current value and its past and future values.

To capture the autocorrelation, the superposition of OU processes defined in (8) is used. Thus, the autocorrelation of each scenario has to be fitted to the function defined in (10). This can be done with any conventional curve fitting algorithm. In this case, a non-linear least squares method, included in the Python package ScipPy [25] is used. The number of decaying exponential and/or damped sinusoidal functions used to fit the autocorrelation can most often be estimated visually or, if not, by trial and error. Further details on this fitting procedure are provided in [19].

Table II shows the fitted parameters for the autocorrelation functions for each scenario. In the table, it is assumed that $\psi_i = 0$ if not provided.

TABLE II: The fitted autocorrelation and probability distribution parameters for the current fluctuations models of Scenario 1 and 2.

Scenario	Autocorrelation Parameters		Standard deviation
1	$w_1 = 0.23$	$\kappa_1 = -5$	$\sigma_X = 0.09266\, u_0$
	$w_2 = 0.32$	$\kappa_2 = -0.2$	
	$w_3 = 0.45$	$\kappa_3 = -0.04$	
2	$w_1 = 0.28$	$\kappa_1 = -5$	$\sigma_X = 0.09702\, u_0$
	$w_2 = 0.18$	$\kappa_2 = -0.2$	
	$w_3 = 0.46$	$\kappa_3 = -0.05$	
	$w_4 = 0.08$	$\kappa_4 = -0.06$	
		$\psi_4 = 0.7$	

In Fig. 1.c, it is shown that there is a correlation between the mean tidal current speed and the standard deviation of the fluctuations. Hence, the standard deviation is dependent on the magnitude of the tidal current speed. The higher the tidal current speed the higher the standard deviation of the fluctuations in the current [5]–[8]. To determine this relationship the mean of the rolling standard deviation as a function of the rolling mean is found as follows:

$$\frac{\sigma_X}{u_0} = \frac{\sum_i^n \sigma_{r_i}/\mu_{r_i}}{n}, \tag{13}$$

where μ_{r_i} and σ_{r_i} are the rolling mean and standard deviation respectively for the i-th time frame of the n time frames of data. In this case the time frame is 10 min. In this way, (13) can give the relation between the tidal current magnitude u_0 an the standard deviation σ_X. The standard deviation for each measured scenario is shown in Table II. In both cases the standard deviation is slightly less than $10\ \%$ of the tidal current magnitude. This value can be subject to the tidal conditions (flood/ebb tides) or the date. This topic is outside the scope of this work but will be considered for future work.

B. Simulations

The data-fitted models presented in Section V-A are now utilized to generate synthetic tidal current speed trajectories whose statistical properties accurately reproduce those of the actual tidal current data sets. With this aim, (8) needs to be integrated. To solve the SDE the Euler-Maruyama integration method is used. Other integration methods for SDEs can be found in [22] but, given the accuracy of the results discussed below, the Euler-Maruyama scheme works well and no higher order method is deemed to be required.

The synthetic models are simulated to produce $1 \cdot 10^6$ data points with the time step 0.01. To test the accuracy of the developed models the statistical properties of the simulated synthetic processes are compared to those of the actual data. These comparisons are carried out in the remainder of this section.

1) Probability Distribution: A Gaussian probability distribution is characterized by its mean (μ) and standard deviation (σ). The mean of the fluctuations is in theory 0 as is the case for both the measured and simulated data as is shown in Table III.

TABLE III: The mean (μ), standard deviation (σ) and the standard deviation of ramps for a 1, 10 and 50 s time step ($\sigma_{f=1\text{s}}$, $\sigma_{f=10\text{s}}$ and $\sigma_{f=50\text{s}}$) for Scenario 1 & 2 measured and simulated.

	Scenario 1		Scenario 2	
	Measured	Simulated	Measured	Simulated
μ	0.0010	0.0013	0.0006	0.0030
σ	0.1723	0.1740	0.1597	0.1569
$\sigma_{f=1\text{s}}$	0.1366	0.1360	0.1360	0.1353
$\sigma_{f=10\text{s}}$	0.2003	0.1989	0.1858	0.1845
$\sigma_{f=50\text{s}}$	0.2410	0.2385	0.2244	0.2213

The standard deviation of the simulated trajectories can be set through the parameter σ_x in (8). Based on the average tidal current speed, u_0, the standard deviation can be set, for example, as shown in Table II. In these simulations the models are assumed to have the standard deviation of the whole data sets shown in Table III. The synthetic simulated current processes capture the standard deviations of the actual measured fluctuations for the two scenarios. The standard

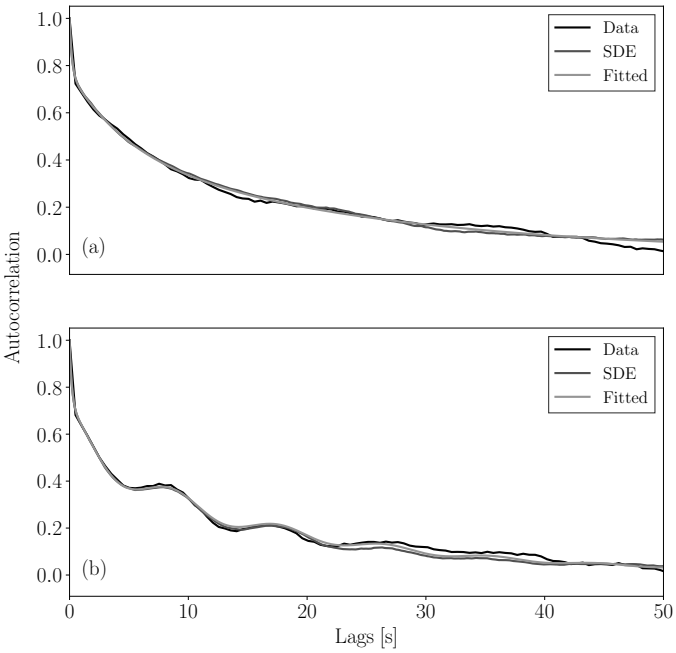

Fig. 2: The autocorrelation of the data set, the fitted autocorrelation function and the autocorrelation of the simulated SDE model for: (a) Scenario 1 and (b) Scenario 2.

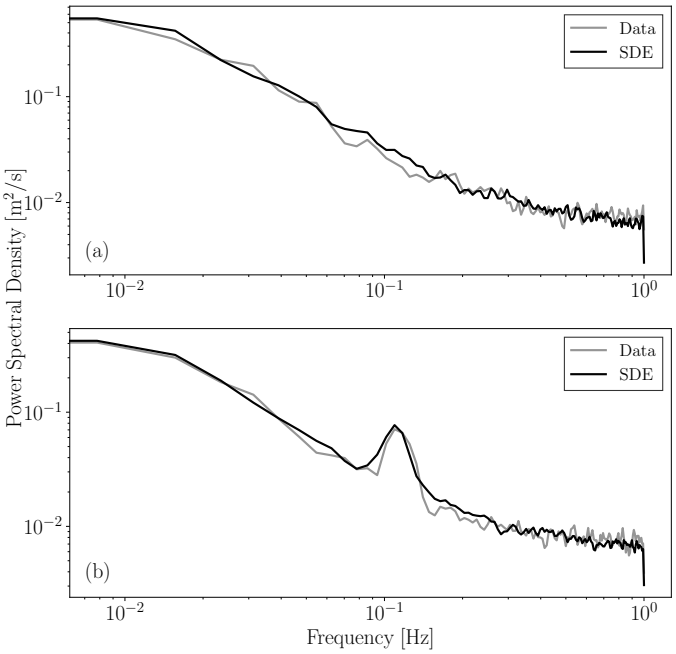

Fig. 3: The power spectral density for the measured data and the SDE simulated time-series for: (a) Scenario 1, (b) Scenario 2.

deviation of the simulated time series is within 2 % error with respect to the standard deviation of the measured data for both scenarios.

The standard deviation of the data of Scenario 1 is slightly bigger than that of Scenario 2. However, these values are not comparable as the two data sets are gathered over different times of the day. What is comparable, however, is the standard deviation as a function of the mean tidal current. With this aim, Table II shows that the standard deviation for Scenario 2 is slightly bigger or about 9.7 % compared to 9.2 % of the mean current for Scenario 1.

2) Autocorrelation: The method presented in Section III is designed to capture the desired autocorrelation. The fitting procedure presented in Section V-A is used here to fit the data to an autocorrelation function that the modeling method can capture. For Scenario 1 the autocorrelation can be captured through the superposition of three OU processes. In this scenario, the fluctuations are primarily due to turbulence. Thus, no periodicity is identified in the autocorrelation. In Fig. 2.a the autocorrelation of the data for Scenario 1 is shown, as well as the fitted autocorrelation function and the autocorrelation of the simulated synthetic time-series derived from the model.

For Scenario 2, periodic behavior driven by the waves in the tidal current is observable in the autocorrelation. Thus, in this case, an additional OU process is needed to capture the periodicity. The autocorrelation of the data for Scenario 2, the fitted autocorrelation function and the autocorrelation of the simulated process are shown in Fig. 2.b.

The behavior of the autocorrelation for Scenario 2 indicates that the waves are periodic with a frequency around 0.1 Hz. In the proposed model, the periodicity is set through the parameter $\psi_4 = 0.7$ rad/s presented in Table II. In particular, for Scenario 2, a frequency of 0.11 Hz, which corresponds to a period of 9 s, has been determined. This matches the specified peak period of the measured data as specified in Section IV.

For both scenarios the model is able to capture the desired autocorrelation. By capturing the autocorrelation the model ensures that the generated stochastic trajectories evolve in time in the same way as the measured time-series. Further statistical comparisons to support this statement are shown in the following subsections.

3) Power Spectral Density: The power spectral density of a time series measures the time series power content versus frequency. It is defined as the Fourier transform of the autocovariance and can be viewed as the frequency-domain equivalent of the autocovariance. Figures 3.a-b show the power spectral densities of the two scenarios measured and simulated. The power spectral densities for both scenarios look similar for most frequencies except around 0.1 Hz, where a spike is visible for Scenario 2. This is the contribution of the waves in the power spectral density of the measured time series as is discussed in Section V-B.2. For both scenarios the simulated processes have spectral densities that have a very similar trend to those shown by the measurement data.

The similarity of the two scenarios can be observed also in the fitted autocorrelation parameters in Table II. The weights w_i differ, but the first three κ parameters are very similar. The fourth process component of Scenario is really modeling the contribution of the wave. Thus, the first three process components can be said to be capturing the turbulence contribution.

4) Ramps: An important aspect of modeling time-series is the ability to capture ramp rates. This is particularly relevant when tidal power fluctuations are considered and that the resulting SDE-based model is able to properly distinguish between ramps and turbulence. Ramp rates are computed as:

$$\Delta_f w_t = w_t - w_{t-f} \tag{14}$$

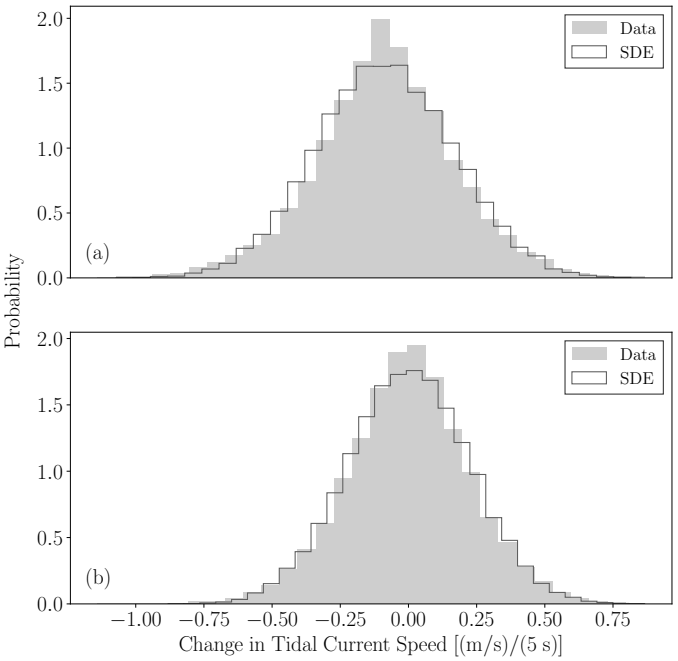

Fig. 4: The histogram of the ramp rates over a 5 s time step for Scenario 1, the measured data and the SDE simulated time series for: (a) Scenario 1 and (b) Scenario 2.

for a time lag f where w_t is the current speed at time t. Then, the probability of getting a certain ramp rate over a time step f can be computed. This is done for a 5 s time step as shown for both scenarios in Fig. 4.a-b. The ramps are shown to be Gaussian and that the model is able to capture the probability of each ramp rate for this time frame. The model is also tested for three other time frames, as shown in Table III. There the standard deviation of ramps with a time step of 1, 10 and 50 s are presented. The results for the simulated time series are close to the measurement data and, thus, the ramp rates of the measurement data are accurately reproduced.

VI. Generated Power

This section presents the current fluctuations model used most commonly in the tidal power studies in the literature. This model will be hereinafter referred to as the Stokes model and is presented in Section VI-A. This model and the proposed model discussed in Section V-B provide the input for the tidal turbine model outlined in Section VI-B. Through this model the turbines power output is modeled. In Section VI-C the equivalent power output for the proposed model and the Stokes model are compared. Concluding remarks on the comparison are provided in Section VI-D.

A. Stokes Model

In the literature on tidal power, short-term fluctuations are assumed to be mainly due to swell waves [11]–[14]. Swell waves are long wavelength waves that originate in a remote region of the ocean and propagate out of their area of generation. Generally, these waves have been modeled using the first order Stokes model representing a random sea-state [26]:

$$u_{\text{swell}}(t) = \sum_{i=1}^{N} a_i \omega_i \frac{\cosh[k_i(h+d)]}{\sinh(k_i d)} \cos[\omega_i t - k_i x + \phi_i], \quad (15)$$

where h is the vertical distance from the sea surface to the hub height of the tidal turbine, positive upwards, and d is the sea depth. ϕ_i are random phases uniformly distributed between 0 and 2π, ω_i is the frequency of the i-th frequency component, k_i is the wave number of the i-th frequency component. With:

$$a_i = \sqrt{2S(\omega_i)\Delta\omega_i} \quad (16)$$

being the amplitude of the i-th frequency component defined from the frequency spectrum, $S(\omega)$, of the waves. In this case, the frequency spectrum used is the JONSWAP spectrum. The wave angular frequency ω_i is within the frequency band $\Delta\omega_i$.

The JONSWAP spectrum is defined as:

$$S(\omega) = \frac{\alpha g^2}{\omega^5} \exp\left(-1.25 \left(\frac{\omega_p}{\omega}\right)^4 \right) \gamma^Y, \quad (17)$$

where ω is the wave angle frequency, g is the acceleration due to gravity, ω_p is the peak frequency of the spectrum and γ is the peak enhancement factor which controls the sharpness of the peak. α is the intensity of the spectrum and can be defined for North Sea applications [15] as:

$$\alpha = 5.058 \left(\frac{H_s}{T_p^2}\right)^2 (1 - 0.287 \ln\gamma), \quad (18)$$

where H_s is the significant wave height, T_p is the peak wave period and

$$Y = \exp\left(-\left(\frac{\omega - \omega_p}{\sqrt{2}\omega_p \sigma_Y}\right)^2 \right), \quad (19)$$

where

$$\sigma_Y = \begin{cases} 0.07 & \text{if } \omega \leq \omega_p \\ 0.09 & \text{if } \omega > \omega_p. \end{cases} \quad (20)$$

The parameters for the Stokes model coupled with the JONSWAP spectrum are set as in the swell wave case studied in [11]. There the number of frequency components and the frequency range used for (16) was not specified. In this work, the frequency range is set to $[\omega_{\min}, \omega_{\max}] = [0.1, 1]$ rad/s and the number of frequency components is $N = 30$. Also, the significant wave height is set to $H_s = 1.9$ m and the peak wave period is set to be $T_p = 9$ s as for the measured data in Scenario 2.

The randomness in the sea-state is expressed through the JONSWAP spectrum, as presented in (17). Other spectrum such as the Pierson-Moskowitz and the Ochi-Hubble spectrum can also represent the random sea-state of the location. However, the JONSWAP spectrum is the most common choice in the literature [11]–[14]. Note that the parameters of this spectrum, such as γ, are location dependent. The values of the wave angular frequency of the spectrum for the measurement location are not available to the authors. Thus, the parameters of the JONSWAP spectrum considered in this paper do not represent the specific sea-state of the measurement location discussed in the case study.

B. Tidal Turbine Model

The modeled current speed is the input to the tidal turbine model. The tidal turbine model determines the mechanical power for the generator rotor based on the input current speed. The turbine power output is modeled as:

$$P_{\text{turbine}} = \frac{1}{2} \cdot \rho_{\text{water}} \cdot A \cdot C_p(\lambda, \beta) \cdot V^3, \tag{21}$$

where ρ_{water} [kg/m^3] is the sea water density, A [m] is the swept area of the rotor and V [m/s] is the equivalent current speed. $C_p(\lambda, \beta)$ is the power coefficient of the blades which is a function of the tip speed ratio (λ) and the blade pitch angle (β [deg]). The tip speed ratio is:

$$\lambda = \frac{\omega_r \cdot R}{V}, \tag{22}$$

where ω_r [m/s] is the rotational speed of the tidal current turbine.

The tidal turbine modeled in this example is a three-bladed horizontal-axis 1.5 MW turbine. The power coefficient is modeled as [27]:

$$C_p(\lambda, \beta) = c_1 \left(\frac{c_2}{\lambda_i} - c_3 \cdot \beta - c_4 \right) \exp(-c_5/\lambda_i) + c_6 \cdot \lambda, \tag{23}$$

where the power coefficient parameters are set to: $c_1 = 0.35$, $c_2 = 100$, $c_3 = 0.4$, $c_4 = 3.93$, $c_5 = 17.25$ and $c_6 = 0.013$ and

$$\frac{1}{\lambda_i} = \frac{1}{\lambda + 0.08 \cdot} - \frac{0.035}{\beta^3 + 1}. \tag{24}$$

C. The Output Power

The Stokes model and the proposed model (for Scenario 2) are utilized to generate the synthetic tidal current processes shown in Figs. 5.a-b, respectively. From Fig. 5 it can be observed that the tidal current variations are assumed to be off a larger scale in the Stokes model than the proposed model.

The equivalent power output for both the Stokes model (gray line) and the proposed model (black line) are shown in Fig. 5.c. The Stokes model generates a power output which fluctuates in the worst case almost the full range of the output power of the tidal turbine within 10 s, that is 1.5 MW. On the other hand, the proposed model produces a power output where the power does ramp up and down between $0.5 - 1.3$ MW over approximately the same time frame.

D. Remarks

Figure 5 shows that the Stokes and the proposed models produce very different tidal current speeds. This is to be expected as the two models have different goals. The Stokes model considers only the effect of waves and neglects turbulence. Moreover, such a model does not represent the location or the sea-state. The proposed model, on the other hand, is aimed at accurately reproducing the statistical properties of a specific location based on measurement data that include both waves and turbulence. The data for Scenario 2 has an underlying wave component that affects the current speed as shown in Fig. 2-3. However, the effect of the turbulence on the current speed results in the wave component not being prominent.

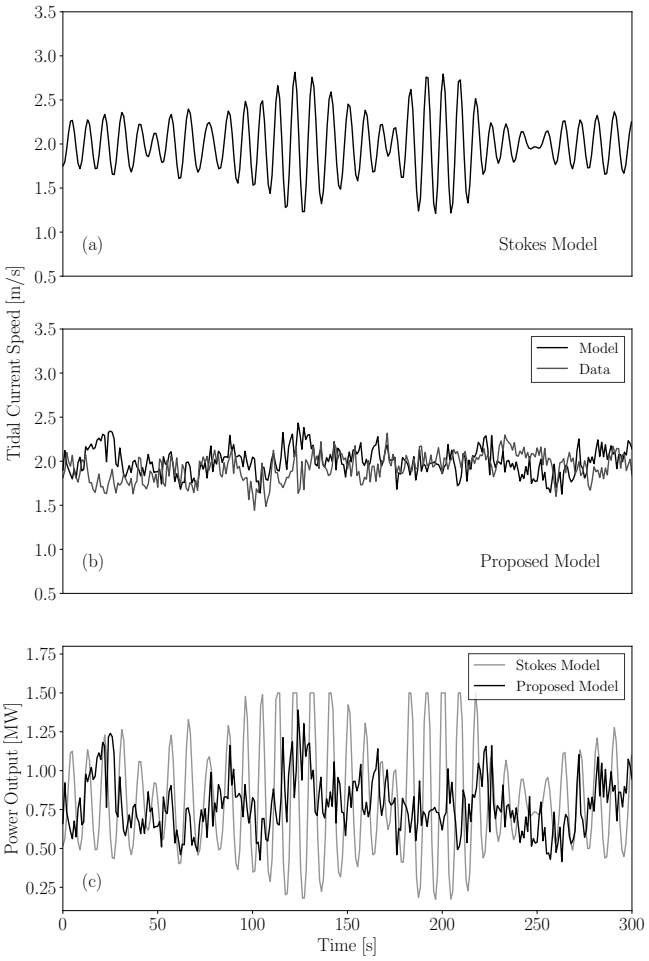

Fig. 5: (a) Generated synthetic tidal current speed using the Stokes model. (b) Generated synthetic tidal current speed using the proposed model and the measured data time series for Scenario 2. (c) Equivalent power output generated using the turbine model in (21).

Despite their differences, both models are useful. If measurements are available, the proposed model is the better option as it captures the combined effect of waves and turbulence of the sea-states for a specific site. The Stokes model, on the other hand, is a suitable option whenever measurement data are not available.

VII. Conclusions

The paper deals with the modeling of tidal current speed for short-term analysis. A SDE-based technique is utilized to model current fluctuations. The models are defined from the autocorrelation and probability distribution of current measurements. The proposed modeling approach is general and can be systematically applied to model any sea-state, if a sufficiently large set of current speed measurements is available.

In the case study, two scenarios are considered. In the first scenario, fluctuations are due exclusively to turbulence whereas, in the second scenario, fluctuations are due to turbulence and waves. As expected, the proposed SDE-based models are able to capture the statistical properties of the

measured data for both scenarios. Finally, the equivalent power output of the tidal turbine is simulated using the proposed model and the Stokes model coupled with the JONSWAP spectrum. It is shown that the power output for these two models is very different. This highlights the importance of using measurements to build site specific models that consider turbulence and wave scenarios.

Future work will focus on the effect of different tidal conditions on the standard deviation and the probability distribution of the turbulence. We also plan to utilize the proposed model to study the impact of marine current generation on power system short-term dynamics.

ACKNOWLEDGEMENTS

Field measurements from the EMEC tidal test site were acquired under the ReDAPT project (2010-2015) which was co-funded by the Energy Technologies Institute (ETI), UK.

We thank Brian Sellar, with the University of Edinburgh for his assistance with the data and comments that greatly improved the manuscript.

REFERENCES

[1] R. Alcorn and D. O'Sullivan, Eds., *Electrical Design for Ocean Wave and Tidal Energy Systems*, ser. Energy Engineering. Institution of Engineering and Technology, 2013.

[2] Ocean Energy Forum, "Ocean energy strategic roadmap: Building ocean energy for Europe," Tech. Rep., 2016.

[3] MeyGen Array Sets Global Record for Harnessing Tidal Power (September 2018). [Online]. Available: https://www.powermag.com/meygen-array-sets-global-records-for-harnessing-tidal-power/

[4] T. Thiringer, J. MacEnri, and M. Reed, "Flicker evaluation of the SeaGen tidal power plant," *IEEE Transactions on Sustainable energy*, vol. 2, no. 4, pp. 414–422, 2011.

[5] I. Milne, R. Sharma, R. Flay, and S. Bickerton, "Characteristics of the turbulence in the flow at a tidal stream power site," *Philosophical Transactions of the Royal Society A: Mathematical, Physical and Engineering Sciences*, 2013.

[6] J. Thomson, B. Polagye, M. Richmond, and V. Durgesh, "Quantifying turbulence for tidal power applications," in *IEEE Oceans, Seattle*, 2010.

[7] J. Filipot, M. Prevosto, C. Maisondieu, M. Le Boulluec, and J. Thomson, "Wave and turbulence measurements at a tidal energy site," in *IEEE/OES Eleveth Current, Waves and Turbulence Measurement (CWTM)*, 2015.

[8] J. Thomson, B. Polagye, V. Durgesh, and M. C. Richmond, "Measurements of turbulence at two tidal energy sites in Puget Sound, WA," *IEEE Journal of Oceanic Engineering*, vol. 37, no. 3, pp. 363–374, 2012.

[9] B. Sellar, G. Wakelam, D. Sutherland, D. Ingram, and V. Venugopal, "Characterisation of tidal flows at the European marine energy centre in the absence of ocean waves," *Energies*, vol. 11, no. 1, p. 176, 2018.

[10] M. Arnold, F. Biskup, and P. W. Cheng, "Load reduction potential of variable speed control approaches for fixed pitch tidal current turbines," *International Journal of Marine Energy*, vol. 15, pp. 175–190, 2016.

[11] M. B. Anwar, M. S. El Moursi, and W. Xiao, "Dispatching and frequency control strategies for marine current turbines based on doubly fed induction generator," *IEEE Transactions on Sustainable Energy*, vol. 7, no. 1, pp. 262–270, 2016.

[12] Z. Zhou, M. Benbouzid, J. F. Charpentier, F. Scuiller, and T. Tang, "A review of energy storage technologies for marine current energy systems," *Renewable and Sustainable Energy Reviews*, vol. 18, pp. 390–400, 2013.

[13] K. Ghefiri, I. Garrido, S. Bouallègue, J. Haggège, and A. Garrido, "Hybrid neural fuzzy design-based rotational speed control of a tidal stream generator plant," *Sustainability*, vol. 10, no. 10, p. 3746, 2018.

[14] Z. Zhou, F. Scuiller, J. F. Charpentier, M. E. H. Benbouzid, and T. Tang, "Power smoothing control in a grid-connected marine current turbine system for compensating swell effect," *IEEE Transactions on Sustainable Energy*, vol. 4, no. 3, pp. 816–826, 2013.

[15] K. Hasselmann, T. Barnett, E. Bouws, H. Carlson, D. Cartwright, K. Enke, J. Ewing, H. Gienapp, D. Hasselmann, P. Kruseman *et al.*, "Measurements of wind-wave growth and swell decay during the Joint North Sea Wave Project (JONSWAP)," *Ergänzungsheft 8-12*, 1973.

[16] Recommend Practice DNV-RP-C205 - Environmental conditions and environmental loads (April, 2014). [Online]. Available: https://rules.dnvgl.com/docs/pdf/DNV/codes/docs/2014-04/RP-C205.pdf

[17] K. Wang and M. L. Crow, "Numerical simulation of stochastic differential algebraic equations for power system transient stability with random loads," in *IEEE PES General Meeting, Detroit*, 2011.

[18] R. Zárate-Miñano, M. Anghel, and F. Milano, "Continuous wind speed models based on stochastic differential equations," *Applied Energy*, vol. 104, pp. 42–49, 2013.

[19] G. M. Jónsdóttir and F. Milano, "Data-based continuous wind speed models with arbitrary probability distribution and autocorrelation," *Renewable Energy*, 2019.

[20] M. Anvari, B. Werther, G. Lohmann, M. Wächter, J. Peinke, and H.-P. Beck, "Suppressing power output fluctuations of photovoltaic power plants," *Solar Energy*, vol. 157, pp. 735–743, 2017.

[21] G. Jónsdóttir and F. Milano, "Modeling solar irradiance for short-term dynamic analysis of power systems," *IEEE PES General Meeting, Atlanta*, 2019.

[22] P. E. Kloeden, E. Platen, and H. Schurz, *Numerical solution of SDE through computer experiments*. Springer Science & Business Media, 2012.

[23] "Tidal Current of the Brittany Western Coast: From Gouvlen to Penmarc'h Grench Navy Hydrographic and Oceanographic Service (SHOM)," Paris, France, 1994.

[24] Met-Ocean Data Science for Offshore Renewable Energy Applications, (2017). [Online]. Available: http://redapt.eng.ed.ac.uk/index.php

[25] SciPy Reference Guide. Release 0.13.0 (accessed 23 August 2018). [Online]. Available: https://docs.scipy.org/doc/scipy-0.13.0/scipy-ref.pdf

[26] Y. Goda, *Random seas and design of maritime structures*. World Scientific Publishing Company, 2010, vol. 33.

[27] M. C. Sousounis, J. K. Shek, and B. G. Sellar, "The effect of supercapacitors in a tidal current conversion system using a torque pulsation mitigation strategy," *Journal of Energy Storage*, vol. 21, pp. 445–459, 2019.

Guðrún Margrét Jónsdóttir (S'14) recieved a BSc in in Electrical and Computer Eng. for the University of Iceland in 2013 and a MSc in Electric Power Eng. from KTH, Stockholm, Sweden in 2015. She worked as a research engineer at KTH SmarTS Lab from 2015 to September 2016 when she began a Phd in the University College Dublin, Ireland. Her research interests include the stochastic modeling of renewable energy sources in power systems, specifically wind, solar and tidal.

Federico Milano (F'16) received from the Univ. of Genoa, Italy, the ME and Ph.D. in Electrical Eng. in 1999 and 2003, respectively. From 2001 to 2002 he was with the Univ. of Waterloo, Canada, as a Visiting Scholar. From 2003 to 2013, he was with the Univ. of Castilla-La Mancha, Spain. In 2013, he joined the Univ. College Dublin, Ireland, where he is currently Professor and Head of Electrical Engineering. His research interests include power system modelling, control and stability analysis.